Resolution acuity for equiluminant gratings of S-cone positive or negative contrast in human vision

Margarita B. Zlatkova
Visual Science Research Group, School of Biomedical Sciences, University of Ulster, Coleraine, Northern Ireland, UK

Angel Vassilev
Institute of Neurobiology (Former Institute of Physiology), Bulgarian Academy of Sciences, Sofia, Bulgaria

Roger S. Anderson
Visual Science Research Group, School of Biomedical Sciences, University of Ulster, Coleraine, Northern Ireland, UK

We measured resolution acuity separately for gratings with positive (+S) and negative (−S) S-cone contrast at different eccentricities in the temporal retina to determine if the resolution performance is limited by a single bipolar opponent mechanism. Gratings were modulated from an achromatic background in either the 90 or 270 deg direction in DKL space. Two additional directions were tested to examine the effects of increased lens yellowing and macular pigment absence in the periphery. The gratings used slow temporally rising hue (co-sinusoidal step) to aid selective S-cone ON or OFF stimulation. Resolution acuity was measured using different luminance ratios of the grating bars with the background around the equiluminant point. The data displayed a plateau where the acuity was minimal and mediated by the sparse S-cone pathway, with observer performance rising on either side. The acuity at the minimum was consistently higher for +S gratings than −S gratings beyond 10 deg eccentricity. Above the resolution limit, an aliased pattern was detected for both types of gratings, indicating that the resolution acuity was limited by the density of postreceptoral neurons. The results suggest that the resolution of gratings with opposite S-cone contrast polarity is limited by separate and rectified mechanisms of different distribution.

Keywords: color vision, resolution, color opponency, S-cone ON and OFF pathways, equiluminance

Citation: Zlatkova, M. B., Vassilev, A., & Anderson, R. S. (2008). Resolution acuity for equiluminant gratings of S-cone positive or negative contrast in human vision. *Journal of Vision, 8*(3):9, 1–10, http://journalofvision.org/8/3/9/, doi:10.1167/8.3.9.

Introduction

It is now generally accepted that, at an early stage of color encoding, the signals from the three kinds of cones are combined in an opponent fashion to form two chromatic channels, loosely referred to as "red-green" and "blue-yellow." In the red-green channel, signals from long wavelength (L) cones are opposed by the signals from middle wavelength (M) cones, while in the blue-yellow channel, the signals from short wavelength (S) cones are opposed by the sum of L- and M-cone input. The widely accepted concept that these two cone-opponent mechanisms are bipolar, that is, each opponent channel responds with a difference signal of opposite sign to two complementary colors, red-green or blue-yellow (e.g., Kaiser & Boynton, 1996), has recently been questioned. Stimuli that give rise to responses of opposite signs may be processed by two different and independent mechanisms instead of a single bipolar mechanism, or separate signals may arise for each pole of the opponent mechanism, for example, "red," "green," "blue," or "yellow" (Sankeralli & Mullen, 2001). The first suggestion of this kind of separated "unipolar" cone-opponent processing comes from an influential study using habituation saw-tooth modulation (Krauskopf, Williams, & Heeley, 1982). It was shown that the thresholds for step changes in opposite chromatic directions are selectively elevated when the habituation modulation changes its sign. Evidence for separate rectified opponent mechanisms comes also from masking studies (McKeefry, Abdelaal, Barrett, & McGraw, 2005; Sankeralli & Mullen, 2001) and adaptation studies using steady and transient adaptation conditions (McLellan & Eskew, 2000).

In our previous studies, we have shown a relative enlargement of the area of complete spatial summation

doi: 10.1167/8.3.9 Received June 27, 2007; published March 12, 2008 ISSN 1534-7362

(Ricco's area) in the retinal periphery for S-cone decrements compared to S-cone increments (Vassilev, Mihaylova, Racheva, Zlatkova, & Anderson, 2003; Vassilev, Zlatkova, Manahilov, Krumov, & Schaumberger, 2000). This asymmetry supports the notion of separate S-cone driven pathways that respond to either S-cone increments or decrements and suggests that they have different spatial characteristics. Calculations based on morphological data (Curcio et al., 1991) have shown that, at an eccentricity of 20 deg, the area of complete spatial summation for S-cone increments covers about 40 S cones while in the case of decrements it involves twice as many, 90 S cones on average. The increased summation for S-cone decrements might be related to larger dendritic fields of the cells that convey S-OFF signals compared to the cells that convey S-ON signals and, consequently, lower density of S-OFF cells compared with S-ON cells. This inference can be based on the principle that "all retinal ganglion cell classes are likely to produce an efficient and economical tiling of the retina with their dendritic fields" (Wassle & Boycott, 1991). There are several problems for the speculations about cell density based on the summation area. The relation between Ricco's area and the retinal anatomy is not clear. We have recently reported that a close correlation exists across the retina (Vassilev, Ivanov, Zlatkova, & Anderson, 2005) between Ricco's area for S-cone increments and the dendritic-field size of the small bistratified cells known as S-ON retinal ganglion cells (Dacey & Lee, 1994). Unfortunately, there are still no consistent data on the morphology of the neural pathways conveying S-OFF signals with which to perform similar comparisons for the S-cone decrements. Any assumption about lower cell density of the pathway conveying S-OFF signals will be dependent on the coverage factor and other considerations, for example, how well Ricco's area correlates with the dendritic field size for different cells types, which is currently unknown. In view of the above problems we decided to use a more direct method that would allow us to make inferences about the density of the cells that respond to S-cone positive and S-cone negative signals.

The method is based on sampling theory and numerous previous studies of detection/resolution acuity. These studies have shown that, while resolution acuity for achromatic stimuli in the fovea is principally limited by the optics of the eye, peripheral resolution is limited by the sampling density of the responding ganglion cells (Anderson, Wilkinson, & Thibos, 1992; Thibos, Cheney, & Walsh, 1987; Thibos, Walsh, & Cheney, 1987). More recently, this has also been shown to be the case for S-cone isolating gratings in both the fovea and periphery, resolution being significantly lower than the optical limit and displaying close correspondence with the density of the ganglion cells with S-cone ON input across the visual field (Anderson, Zlatkova, & Demirel, 2002; for a review, see Calkins, 2001). We assume therefore that measures of chromatic grating resolution at different eccentricities indicate how responding-cell-population density changes for grating stimuli with S-cone positive or S-cone negative contrast. To this end, we measured resolution acuity for stimuli that were chosen to selectively stimulate either the blue or the yellow pole of the blue-yellow opponent channel, by creating either positive or negative S-cone contrast.

Methods

Subjects

Two of the authors (RSA, age 38, and MBZ, age 55) participated as observers in all experiments. An additional observer (JL, age 21), who was naïve to the aims of the experiment, was also tested in some experiments. All participants had foveal corrected Snellen acuity of 6/6 and normal color vision as assessed by The City University Colour Vision Test (3rd ed., 1998). They underwent full ophthalmic examination, which did not reveal any ocular abnormalities. All participants were optically corrected for the viewing distance. In addition, the off-axis astigmatism was corrected at the peripheral location of 20 deg eccentricity, by measuring the refractive error using retinoscopy and placing a trial lens, including a near addition for working distance, in front of the eye. All observers used their right eye in all experiments; the left eye was covered with a black patch.

Stimuli

The stimuli were sinusoidal gratings presented on a 21″ CRT color monitor (Sony GDM-500) driven by a Visual Stimulus Generator VSG2/3 graphic card (Cambridge Research System, Rochester, UK) at a spatial resolution of 1024 × 768 pixels and a frame rate of 100 Hz. The screen size was 32° × 25°. The monitor guns' output was linearized using VSG calibration software (Cambridge Research System, Rochester, UK). A linearity check was performed weekly. The stimuli were presented on an achromatic monitor background with chromaticity coordinates $x = 0.31$, $y = 0.316$, CIE 1931 (illuminant C) and with a luminance of 13 cd/m^2. The chromaticity of the gratings was modulated from this background along either 90 or 270 deg in the equiluminant plane of DKL color space to produce either 80% positive S-cone contrast (+S grating) or 80% negative S-cone contrast (−S grating) without altering the L-cone and M-cone contrast (constant LM axis). This was the maximum contrast attainable for the present background under equiluminant conditions. The gratings were also modulated along additional axes, chosen to maximize the S-cone modulation while keeping LM contrast constant at peripheral locations, to take into account the lack of macular pigment at higher eccentricities and assuming age variations in lens optical density (OD).

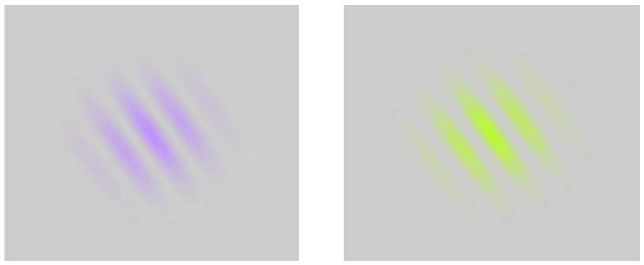

Figure 1. Examples of gratings with S-cone positive (left) and S-cone negative (right) contrast. The gratings are shown in one of the two possible oblique orientations (45 or 135 deg) used in the experiment.

The grating detection and resolution acuity were measured for both + S and −S gratings across the temporal horizontal retinal meridian at 2, 5, 10, and 20° eccentricity and at 13° eccentricity in the 45 deg oblique meridian. This latter location was chosen because, according to subjective reports, the gratings presented there appeared to have strong chromatic contrast. The sinusoidal gratings were presented in 2D circular Gaussian windows (Gabor patches). The spread parameter σ was scaled with eccentricity to ensure that at least three full cycles could be seen at those spatial frequencies close to individual acuity. Thus, the spread parameter of the Gabor function was 0.5 deg at 2° eccentricity, 1 deg at 10° eccentricity, and 2 or 2.5 deg at 20° eccentricity. The gratings had slow temporally rising contrast (co-sinusoidal step, rise time 0.5 s) to minimize temporal transients and to aid selective S-cone ON or OFF stimulation. This type of presentation produced slowly increasing (for +S gratings) or decreasing (for −S gratings) S-cone signal created by the S-cone varying bars of the grating. Figure 1 shows the typical appearance of both grating types on the monitor. In this example, the gratings orientation is 135 deg, which is one of the two alternative orientations (45 or 135 deg) used in the experiment (see "Procedure" section).

The achromatic bars had the same luminance and chromaticity as the background and remained unchanged during the stimulus presentation. The stimulus presentation was terminated by the subject's response. Viewing was monocular with a natural pupil. Head position was stabilized by a forehead and chin support. The fixation target consisted of two small, closely spaced, vertically aligned squares, and the observer was instructed to fixate the central gap. The stimulus was always presented at the same location on the screen and eccentricity was changed by moving the fixation target. The viewing distance was 65 cm in all experiments.

Calculation of S-cone varying axis

The luminance and all radiometric and colorimetric characteristics of the test and background were measured at the eye position using a spectrophotometer (Spectrascan PR-650; Photo Research, Inc., Chatsworth, CA, USA). The luminance and the color coordinates were checked before each daily session. The radiance spectra of the monitor phosphors were measured in 4 nm step, and the cone excitations created by the background were calculated by convolving the spectral distributions of the three phosphors outputs with Smith and Pokorny cone fundamentals (Smith & Pokorny, 1975). R, G, and B modulation depths needed to produce a LMS contrast vector in the equiluminant plane (0, 0, and 0.8) were then calculated. The cone contrast was calculated as $C = (CE_s - CE_b)/CE_b$, where CE_s is cone excitation due to the stimulus and CE_b is cone excitation due to the background. Figure 2 (left graph) shows the spectra of +S and −S stimuli, modulated either along 90 or 270° axis, along with the spectrum of the background.

The variations in pre-retinal media with age and eccentricity might introduce artefacts since the calculated tritanopic (S-cone varying) axis is based on the 2 deg Smith and Pokorny (1975) cone fundamentals and Judd luminosity function (1951) for standard observer. These artefacts would create a contrast in L and M cones and would change the S-cone contrast (Cottaris, 2003; Smith & Pokorny, 1995). The individual variations in the pre-retinal media would also be a factor. With this in mind, we introduced two additional chromatic axes shown in Figure 2 (right graph). They were created by (a) removing the macular pigment transmission spectrum from the cone fundamentals to reflect the lack of macular pigmentation in the periphery (axis 1) and (b) by modifying the cone fundamentals assuming a denser lens spectrum (axis 2). Individual measurements of macular pigment OD and lens OD were obtained previously for observers RSA and MBZ using heterocromatic flicker photometry to measure macular pigment OD (Werner, Donnelly, & Kliegl, 1987) and van Norren and Vos's (1974) approach to measure lens OD. Since the peak macular pigment OD for both observers (RSA, 0.41, and MBZ, 0.27) was close to the peak OD of the standard observer (0.35), the individual variations in the macular pigment were neglected, and the standard OD spectrum was used in the calculations. The lens OD

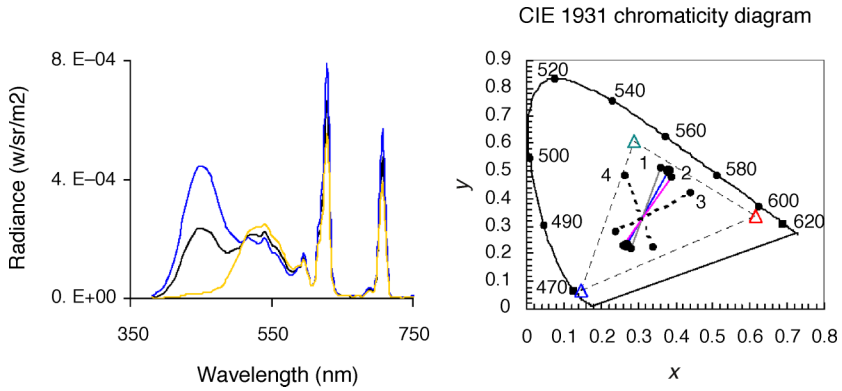

Figure 2. Specification of the chromaticity of stimuli used in the experiment. Left: Spectral radiance distributions of the background (black curve) and of the tritanopic pair: 90 deg (blue curve) and 270 deg (yellow curve). Right: The location of the chromatic axes tested in the CIE (1931) XYZ chromaticity diagram. The triangular area represents the available color gamut. The location of the background (illuminant C, $x = 0.31$, $y = 0.316$) is represented at the point of intersection of the axes. The central axis (blue) is the foveal tritanopic line ($x = 0.27$, $y = 0.23$; $x = 0.38$, $y = 0.5$). Two additional axes were tested: line 1 (grey) on the left assuming a lack of macular pigment ($x = 0.28$, $y = 0.22$; $x = 0.36$, $y = 0.51$) and line 2 (pink) on the right assuming a denser lens ($x = 0.26$, $y = 0.23$; $x = 0.39$, $y = 0.48$). Axes 3 and 4 are explained in the text.

estimate at 430 nm for each observer was consistent with the typical values for his/her age (RSA, 0.58, and MBZ, 0.71). To determine what effect a denser lens may have on the results, axis 2 was calculated using the equation from Pokorny, Smith, and Lutze (1987) to represent a lens density spectrum for age 60. The denser lens correction of axis 1 resulted in a rotation of this axis back to the foveal tritanopic line, thus only axes 1, 2, and the standard tritanopic axis were used in this experiment. Axis 2 was used at 2 deg eccentricity and axis 1 was used at 13 and 20 deg eccentricity together with the foveal tritanopic line.

We next verified the S-cone and L- and M-cone contribution to the three chromatic axes under conditions of S-cone bleach. If an equiluminant grating modulated along these axes creates only S-cone contrast with L- and M-cone contrast remaining zero, the grating should be undetectable when the S cones are bleached. We tested this possibility by measuring the detection of equiluminant +S and −S gratings after 1 min exposure to an intensive blue light to bleach the S cones. The blue light was produced by a slit lamp BM-900 (Haag-Streit, Bern, Switzerland) and cobalt blue filter (maximum intensity at 450 nm). The gratings were presented at maximal contrast on the monitor at a spatial frequency just below the acuity threshold in the fovea or at 20 deg temporal retina. A two-alternative temporal forced choice procedure was used to measure the contrast detection. The standard tritan axis and axis 2 were used in the fovea, and all three axes were used at 20 deg. No contrast was seen for +S or −S gratings until 3 min after adaptation for any of the three chromatic axes at both locations. After that time the chromatic contrast of the gratings was slowly restored. We also tested gratings modulated along two chromatic axes that produce 20% L- and M-cone contrast (axis 3 and 4). The gratings remained readily detectable immediately following the exposure to the bleaching light. All chromatic axes used in the experiments are indicated in the CIE 1931 chromatic diagram in Figure 2.

Procedure

Equiluminance adjustment and S-cone isolation

Before commencing data collection, a heterochromatic flicker photometry (HFP) procedure was used to create roughly subjectively equiluminant stimuli at each eccentricity tested. The gratings used in the experiments flickered at 14 Hz at 2°, 5°, and 10° eccentricity and at 11 Hz at 13° and 20° eccentricity. The observers adjusted the luminance of the chromatic (S-cone varying) bars until a region of minimum flicker was found. The starting luminance was randomly chosen. To better estimate the luminance, or the range of luminances, where the gratings look equiluminant and the acuity is mediated by the S-cone system, we measured resolution acuity using small step differences in the luminance ratio between the S-cone varying bars and the background at each eccentricity. When the luminance component increases, the grating will begin to be resolved by the achromatic system, mediated by L and M cones, and high acuity will result. When the grating is equiluminant, the acuity will be mediated by the sparse S-cone system and will be reduced substantially. By changing the luminance of the S-cone varying bars in relation to the background, we can find a point or a region where the acuity displays a performance minimum and is therefore mediated by the S-cone pathway.

Resolution acuity

The general procedure for measuring the resolution acuity was a two-alternative forced choice orientation identification (45 or 135 deg oblique) and a staircase method. The data collection began after 10 min of dark adaptation followed by 3 min adaptation to the monitor background. The grating was presented on each trial in one of the two orientations (tilted "right" or "left") randomly and with equal probability. The observers had to respond to orientation by pressing the appropriate button. The starting spatial frequency was suprathreshold. Three correct responses resulted in an increase (10%) in spatial frequency and a single incorrect response resulted in a decrease (10%) in spatial frequency. No feedback was given, and the subjects were encouraged to guess if unable to identify the grating orientation. Resolution acuity was calculated as the mean of six reversals of the staircase. Acuity for each condition was measured in five sessions, run on separate days, and the mean values and standard deviations were calculated. All three observers participated.

Comparison of detection and resolution acuity: Signal detection method

Detection and resolution acuity were separately measured using signal detection rating procedure (Green & Swets, 1966; Nachmias & Steinman, 1963) for both tasks. We chose this method to measure detection and resolution performances, which are intrinsically different, using the same criterion-free procedure for both tasks (Thomas, 1985). Only one location at 20 deg eccentricity was tested. The acuity was obtained at a fixed luminance ratio that yielded the lowest resolution acuity for both +S and −S gratings as described in the previous paragraph. Observers RSA and MBZ participated. In the detection task, the gratings were presented on approximately half of the trials; the rest were noise trials. Signal and noise trials were randomly intermixed. The signal trials contained gratings presented at one of three possible spatial frequencies chosen to cover the range of clearly resolvable to nearly nonresolvable. The spatial frequency of the grating varied in a random manner. All other conditions were the same as those in the resolution acuity experiment. The noise probe contained a Gaussian patch (blob) of the same size as the gratings and of chromaticity equal to the average chromaticity of the grating. It was shown in a preliminary test that this patch was indistinguishable from a Gabor patch of spatial frequency above the threshold for detecting the aliased pattern. The acuity for +S and −S gratings was measured in separate sessions. In each trial, the observers had to rate their degree of certainty that the stimulus differs from a uniform field. The observers had to select one of five possible ratings from 0 to 80, where a rating of zero represented a high certainty that no contrast had been present in the stimulus patch and a rating of 80 represented a high certainty that a contrast had been presented. The intermediate categories (20, 40, and 60) represented a degree of certainty that varied between these two extremes.

In the resolution task, the signal probe contained the grating presented at one of three spatial frequencies spanning the range from veridical to nonveridical (aliased) values. The noise probes constituted gratings of spatial frequency above the resolution limit but still visible (aliased). In preliminary tests it was verified that the grating in the noise probes always looked aliased to the observer. The observer's task was to rate their certainty that the grating presented look veridical. The same scale from 0 to 80 was employed.

The data for detection and resolution tasks were obtained in separate daily sessions. Each daily session consisted of two blocks for +S and −S acuity. The number of trials in each block varied between 260 and 340. ROC curves were constructed from subject ratings, averaged over three to four blocks of trials. The three spatial frequencies were presented in random order in a single block of trials. The order of block presentation was random and a different order was used for each observer. The area under the ROC curve for each combination of spatial frequency, type of grating, and task was calculated. This area ranged between 50% and 100% and is equivalent to the percentage-correct in a two-alternative forced choice task.

Control experiment: Rod bleach

The background used in all experiments was 2.94 log scotopic Td; according to Aguilar and Stiles (1954), this value is in the region of steep rod threshold rise near rod saturation. However, our stimuli created considerable rod contrast, almost 29%, and thus the rods could potentially contribute to the resolution performance in the retinal periphery. In this control experiment, resolution acuity was measured at the cone plateau to determine if the rods have any effect on the resolution for +S and −S gratings. To bleach the rods, the observers were exposed for 1 min to a bright, 5.1 log scotopic Td white light (CCT 3300 K), size 32 × 32 deg, centered around 20 deg eccentricity. The dark adaptation curve was measured at small intervals after switching off the bleaching light, by presenting a circular test patch on the CRT monitor, 3.4 deg diameter, using white light (illuminant C with a CCT of approximately 6774 K) to determine the cone plateau. The cone plateau began about 3 min after the bleach and lasted almost 5 min. Resolution grating acuity at the cone plateau was then measured at 20 deg eccentricity for observer MBZ. After a 1 min rod bleach, the observer dark-adapted for 4 min and then light-adapted to the monitor background used in the main experiment for 1 min. Equiluminant +S or −S gratings were presented at 20 deg eccentricity during the cone plateau period. The

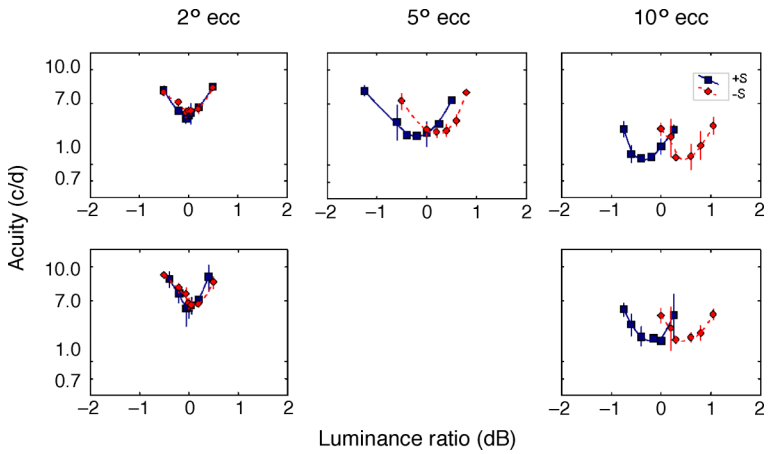

Figure 3. Resolution acuity as a function of luminance ratio between the S-cone varying grating bars and the background. The results are for retinal eccentricities 2, 5, and 10 deg (observer MBZ, top panel) and 2 and 10 deg (observer RSA, bottom panel) along the temporal horizontal meridian. The symbols represent mean resolution acuity for gratings with S-cone positive contrast (blue squares) and with S-cone negative contrast (red diamonds). The vertical bars denote 95% confidence intervals of *SEM* and are seen when the errors are larger than the symbols.

resolution acuity was measured by the same two-alternative forced choice procedure described previously, using a smaller number of reversals. The measurement lasted no more than 2 min. The results for observer MBZ showed no difference in the resolution acuity between bleach and no bleach conditions for both types of grating. The results imply that although the stimuli create some rod contrast, the background used was high enough to desensitize the rods.

Results

Figures 3 and 4 show the resolution acuity for +S and −S gratings for two observers at different eccentricities along the horizontal meridian in the temporal retina.

The resolution acuity is presented as a function of the luminance ratio between the S-cone varying grating bars and the background. A luminance ratio of zero denotes photometric luminance equality. Figure 3 plots the data obtained at 2, 5, and 10 deg eccentricity for observer MBZ (top panel) and the data at 2 and 10 deg for observer RSA (bottom panel).

The results shown in this figure are obtained with stimuli modulated along the foveal tritanopic line. The stimuli modulated along axis 2 which tested the effect of a denser lens on the performance did not produce any systematic changes; results are not shown to save space. The curves demonstrate a U-shape and shift with increasing eccentricity relative to the photometric luminance equality. With the exception of 2 deg eccentricity, the acuity displayed a plateau where both its value and its variance were minimal, and the grating had a clear chromatic appearance, blue-violet in the case of +S gratings and yellow-greenish in the case of −S gratings. The luminance ratio that produced minimum flicker was located in the plateau area, so the grating was also subjectively equiluminant in this area. The acuity increased on both sides of this area, accompanied by an abrupt change in grating appearance. The bars of the gratings looked increasingly sharper and greyish with rising luminance ratio. We assumed that the higher acuity and achromatic appearance is due to the increasing achromatic contrast and that the acuity minimum is mediated by the S-cone pathway. The control experiments with rod and S-cone bleach give additional support that S cones are the only photoreceptors that mediate the resolution of equiluminant +S or −S gratings. In the following text, the term acuity refers to this minimum value, which is mediated by the S-cone pathway. The resolution acuity for +S and −S gratings was compared separately for each subject using a t test. There was no statistically significant difference between the two values at any of the eccentricities up to 10 deg for both subjects (two-tailed t test, $p > .13$).

Figure 4 shows the resolution acuity as a function of the luminance ratio at 13 deg eccentricity (45 meridian) and 20 deg eccentricity (horizontal meridian) in the temporal retina for the three subjects tested.

At these more peripheral locations, the same U-shaped curves were observed with even larger plateaus, especially at 20 deg eccentricity. However, in contrast with the locations at lower eccentricities, +S resolution acuity at the plateau was higher than −S acuity. The difference was consistent and statistically significant for all subjects at both 13 and 20 deg eccentricity (two-tailed t test, $p < .01$). This difference persisted when the gratings were modulated along the additional axis 1, calculated by removing

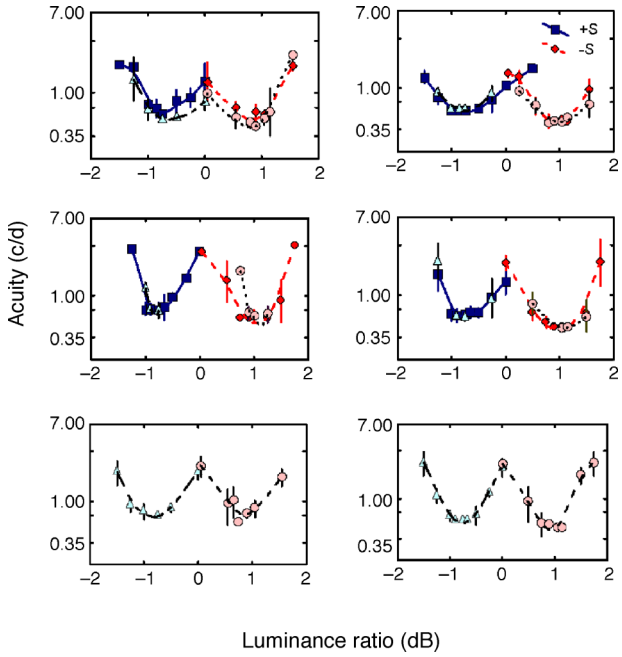

Figure 4. Resolution acuity as a function of luminance ratio between the S-cone varying grating bars and the background for retinal eccentricity 13 deg in the 45 deg meridian (left column) and 20 deg along the horizontal meridian (right column) in the temporal retina. Blue squares show gratings with S-cone positive contrast and red squares show gratings with S-cone negative contrast. Data for the additional axis 1, calculated by removing the macular pigment spectrum, are also shown: light blue triangles represent data for +S gratings and pink circles represent data for −S gratings. The results are for observers MBZ (top panel), RSA (middle panel), and JAL (bottom panel). Note that all observers demonstrate lower acuity for gratings with negative S-cone contrast at these eccentricities.

the macular pigment spectrum from the cone fundamentals. The only effect of the additional axis for both observers was on the width of the plateau and the rate of acuity increase on both sides. Very similar results were obtained with a third naïve observer (JL, age 21) tested only at 13 and 20 deg eccentricity (Figure 4, bottom panel). Only one chromatic axis was tested, that calculated without macular pigment.

Figures 3 and 4 show that both the area of minimum acuity and the equiluminant point shift away from the photometric luminance equality (zero luminance ratio) and that this shift increases with eccentricity. This shift for +S and −S gratings is symmetrical with respect to zero, in agreement with the shift of the maximum of the spectral luminosity curve toward shorter wavelengths, observed in the periphery (Abramov & Gordon, 1977).

According to our initial assumption, the difference between the resolution acuity for +S and −S gratings indicates different sampling density of the responding cells. However, this would only be true if the resolution acuity is limited by the sampling density of the responding cells and not by other factors. The next experiment tested observers ability to detect the aliased pattern at spatial frequencies above the resolution limit for each type of grating. The detection of aliasing would cause a higher acuity for detection since the alias of the grating will be continuously seen above the resolution limit. The results from this experiment are shown in Figure 5, which plots the average area under ROC curves vs. spatial frequency for both the detection and resolution task for each observer. The results for both +S and −S gratings are displayed in the same graph to allow easier comparison.

Because the area under the ROC curve is equivalent to the percentage correct in two-alternative forced choice, the presented curves could be considered psychometric functions, where the performance changes from chance level (50%) to 100% correct level. It is clearly seen that detection performance is better than the resolution performance at all spatial frequencies tested, for both +S and −S gratings. The aliased grating appeared as a highly unstable pattern of chromatic blotches replacing the bars in

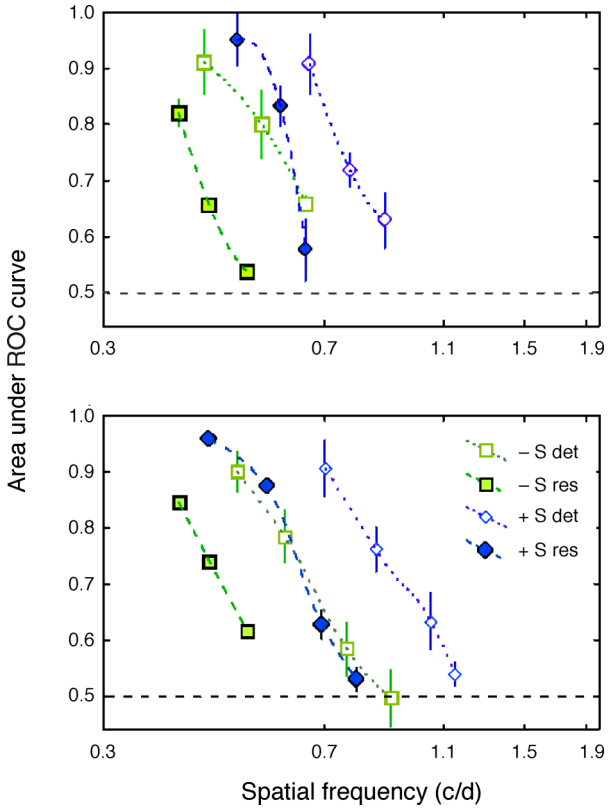

Figure 5. Variation of the area under ROC curve with the spatial frequency for gratings with S-cone positive contrast (blue symbols) and S-cone negative contrast (green symbols) for detection (open symbols) or resolution task (filled symbols). The results are for 20° eccentricity in the temporal horizontal meridian. Each point represents the mean of three or four measurements. Standard error bars are seen when they are larger than the symbols. The results are for observers RSA (top) and MBZ (bottom).

the veridical grating, colored blue-violet or green-yellow for S+ or S- grating. In addition, the detection/resolution curve pair for +S gratings is shifted in parallel toward higher spatial frequency relative to the corresponding curves for −S gratings. This result shows that the +S gratings are better detected and resolved compared to the −S gratings, thus confirming the results for the resolution acuity in an extended range of spatial frequencies.

Discussion

Our results demonstrate that, at retinal locations within 10 deg, the resolution acuity was similar for gratings that differed in their S-cone contrast polarity. However, beyond 10 deg eccentricity, the resolution acuity for gratings with negative S-cone contrast became consistently lower than that for gratings with positive S-cone contrast. An aliased pattern was observed in all locations at spatial frequencies above the resolution limit, giving rise to higher acuity for detection than for resolution. The separation of detection and resolution curves is clearly seen in Figure 5 for both types of grating. The presence of aliasing indicates that the gratings have been undersampled by a neural array with a particular density. The observed difference in +S and −S resolution acuity cannot be explained by optical factors. The simulation of lens yellowing and macular pigment absence did not produce any systematic change in the results. The chromatic aberration and its variation with eccentricity is likely to cause a reduction of the blue grating resolution acuity, or the contrast for detection of the blue aliased pattern (Thibos, 1987), which is opposite to the effect reported here. The acuity values at each location are far below the typical values of the optical modulation transfer function, and the presence of aliasing further confirms that the resolution performance is not limited by optical factors.

The difference between +S and −S grating acuity was observed despite the relatively long duration of our stimuli. The eye movements that occur during the stimulus presentation can compromise the monopolar stimulation, introducing S-cone contrast of opposite sign. We cannot reject the possibility that this factor has affected the magnitude of the observed asymmetry. However, at the peripheral locations where the asymmetry was found, the stimulus spatial frequency was very low, reducing the chance of thresholds being affected by small eye movements.

Our results suggest that the standard blue-yellow cone-opponent mechanism could be considered as composed of two independent and rectified mechanisms that differ in their spatial properties, at least for peripheral vision. If a single opponent mechanism responds to both types of gratings, the resolution would be independent of the stimulus polarity. Both types of grating would be resolved by the same neural mechanism of fixed sampling density. It is therefore reasonable to assume that the resolution of gratings with positive and negative S-cone contrast is mediated by separate mechanisms. Even though the difference between the resolution acuity for S+ and S- gratings is not observed within the central 10 deg, it is reasonable to assume that the same organization of the cone-opponent mechanism exists throughout the retina, albeit with different density distributions of its components. Other studies employing different methods also support the existence of separate mechanisms with S-cone input even in the fovea (McLellan & Eskew, 2000; Sankeralli & Mullen, 2001; Shinomori, Spillman, & Werner, 1999).

The recent study of Sakurai and Mullen (2006) has shown that the contrast sensitivities for the two poles of the blue-yellow opponent mechanism are symmetrical at different peripheral locations. However, their observed symmetry applies to contrast sensitivity rather than resolution. In addition, our previous study (Vassilev et al., 2003) has shown that while for small sizes contrast threshold for S-cone decrements is higher than for S-cone increments, at larger sizes this is not the case. The results of Sakurai and Mullen do not contradict the asymmetries in sensitivity reported in our previous study, since the size of the stimuli they used was large and in the range where detection thresholds for increments and decrements are similar. Asymmetries in the blue-yellow channel have been reported before and have been interpreted as evidence for separate S-cone ON and OFF channels (McLellan & Eskew, 2000; Shinomori et al., 1999). The present results add another asymmetry to the previous data, asymmetry of the sampling density of the cells that mediate these channels. The lower resolution acuity for gratings with negative S-cone contrast suggests that there must be cells with a lower density that limit the resolution of the negative S-cone contrast gratings, at least in the peripheral retina. Anatomical and physiological data show two distinct populations of cells that carry S-cone ON and OFF type signals. In the retina, the cell most often identified as the S-cone ON cell, the small bistratified cell (Dacey, 1993), is sparsely distributed with its density closely corresponding to the predicted resolution acuity values across the retina measured using bipolar blue-yellow gratings (Anderson et al., 2002). Another type of bistratified cell receiving excitatory S-cone input was recently found in the primate retina, thus increasing the diversity of cell populations with S-cone ON input (Dacey & Packer, 2003). The morphology and retinal distribution, as well as the role of these cells in color vision, is still not well known. Similar morphological diversity exists in the cell population receiving S-cone OFF signals. Although it has been known that the S-cone OFF pathway exists in parallel with the S-cone ON pathway (Valberg, Lee, & Tigwell, 1986), cells with S-cone OFF input have been rarely encountered. Dacey et al. (2005) recently reported that a giant melanopsin expressing ganglion cell in primate retina displayed a S-cone OFF response, had a large receptive field, and very low density. Klug, Herr,

Ngo, Sterling, and Schein (2003) reported S-cone OFF connections in the midget bipolar pathway and suggested an S-cone OFF midget pathway. The properties of the cells with S-cone OFF input are still not well understood, and it is not clear if all varieties of cells form a single S-OFF stream to the visual cortex (Szmajda, Buzas, FitzGibbon, & Martin, 2006). There is evidence that the pathways that convey S-cone ON and OFF signals remain segregated up to V1 (Chatterjee & Callaway, 2003). Thus, the neural pathways for separate encoding of S-cone positive and negative signals exist. However, the cells can encode both S-cone positive or negative signals by either excitation or inhibition. This would result in similar acuity or thresholds for both kinds of stimuli. Because of the low maintained discharge of retinal ganglion cells, it is considered unlikely that the inhibition signals are used to encode stimulus features. The process of rectification and the encoding by two monopolar mechanisms on a single bipolar mechanism provides a more efficient way of encoding, independent of a maintained discharge rate and doubling the dynamic range (Howard & Rogers, 1995, p. 72).

The acuities for both kinds of gratings were close to each other up to 10 deg eccentricity, but the acuity for the S-cone negative grating declined faster farther in the periphery. We were not able to register resolution acuity at eccentricities beyond 20° because of the low acuity values that would require too large a stimulus size. There is some evidence that the cells with S-cone OFF input have lower density and larger dendritic fields (Dacey et al., 2005; Szmajda et al., 2006), but since this evidence is still very limited, we do not speculate further about the neural basis of the +S and −S resolution acuity differences and distribution across the retina.

Acknowledgments

This study was supported by a Collaborative Research Initiative Grant from the Welcome Trust (UK).

Commercial relationships: none.
Corresponding author: Margarita B. Zlatkova.
Email: mb.vidinova@ulster.ac.uk.
Address: Vision Science Research Group, School of Biomedical Sciences, University of Ulster, Coleraine BT52 1SA, Co. Londonderry, United Kingdom.

References

Aguilar, M., & Stiles, W. S. (1954). Saturation of the rod mechanism of the retina at high levels of stimulation. *Journal of Modern Optics, 1,* 59–65.

Abramov, I., & Gordon, J. (1977). Color vision in the peripheral retina. I. Spectral sensitivity. *Journal of the Optical Society of America, 67,* 195–202. [PubMed]

Anderson, R. S., Wilkinson, M. O., & Thibos, L. N. (1992). Psychophysical localization of the human visual streak. *Optometry and Visual Science, 69,* 171–174. [PubMed]

Anderson, R. S., Zlatkova, M. B., & Demirel, S. (2002). What limits detection and resolution of short-wavelength sinusoidal gratings across the retina? *Vision Research, 42,* 981–990. [PubMed]

Calkins, D. J. (2001). Seeing with S cones. *Progress in Retinal and Eye Research, 20,* 255–287. [PubMed]

Chatterjee, S., & Callaway, E. M. (2003). Parallel colour-opponent pathways to primary visual cortex. *Nature, 426,* 668–671. [PubMed]

Cottaris, N. (2003). Artifacts in spatiochromatic stimuli due to variations in preretinal absorption and axial chromatic aberration: Implications for color physiology. *Journal of the Optical Society of America A, Optics, Image Science, and Vision, 20,* 1694–1713. [PubMed]

Curcio, C. A., Allen, K. A., Sloan, K. R., Lerea, C. L., Hurley, J. B., Klock, I. B., et al. (1991). Distribution and morphology of human cone photoreceptors stained with anti-blue opsin. *Journal of Comparative Neurology, 312,* 610–624. [PubMed]

Dacey, D. M. (1993). Morphology of a small-field bistratified ganglion cell type in the macaque and human retina. *Visual Neuroscience, 10,* 1081–1098. [PubMed]

Dacey, D. M., & Lee, B. B. (1994). The 'blue-on' opponent pathway in primate retina originates from a distinct bistratified ganglion cell type. *Nature, 367,* 731–735. [PubMed]

Dacey, D. M., Liao, H. W., Peterson, B. B., Robinson, F. R., Smith, V. C., Pokorny, J., et al. (2005). Melanopsin-expressing ganglion cells in primate retina signal colour and irradiance and project to the LGN. *Nature, 433,* 749–754. [PubMed]

Dacey, D. M., & Packer, O. S. (2003). Colour coding in the primate retina: Diverse cell types and cone-specific circuitry. *Current Opinion in Neurobiology, 13,* 421–427. [PubMed]

Green, D. M., & Swets, J. A. (1966). *Signal detection theory and psychophysics*. New York: John Wiley and Sons.

Howard, I. R., & Rogers, B. J. (1995). *Binocular vision and stereopsis*. Oxford: Oxford University Press.

Kaiser, P. K., & Boynton, R. M. (1996). *Human color vision* (2nd ed.). Washington, D. C.: Optical Society of America.

Klug, K., Herr, S., Ngo, I. T., Sterling, P., & Schein, S. (2003). Macaque retina contains an S-cone off midget pathway. *Journal of Neuroscience, 23,* 9881–9887. [PubMed] [Article]

Krauskopf, J., Williams, D. R., & Heeley, D. W. (1982). Cardinal directions of color space. *Vision Research, 22,* 1123–1131. [PubMed]

McKeefry, D. J., Abdelaal, S., Barett, B. T., & McGraw, P. V. (2005). Chromatic masking revealed by the standing wave of invisibility illusion. *Perception, 34,* 913–920. [PubMed]

McLellan, J. S., & Eskew, R. T. (2000). ON and OFF S-cone pathways have different long-wave cone inputs. *Vision Research, 40,* 2449–2465. [PubMed]

Nachmias, J., & Steinman, R. M. (1963). Study of absolute visual detection by the rating-scale method. *Journal of the Optical Society of America, 53,* 1206–1213. [PubMed]

Pokorny, J., Smith, V. C., & Lutze, M. (1987). Aging of the human lens. *Applied Optics, 26,* 1437–1440.

Sakurai, M., & Mullen, K. T. (2006). Cone weights for the two cone-opponent systems in peripheral vision and asymmetries of cone contrast sensitivity. *Vision Research, 46,* 4346–4354. [PubMed]

Sankeralli, M. J., & Mullen, K. T. (2001). Bipolar or rectified chromatic detection mechanisms? *Visual Neuroscience, 18,* 127–135. [PubMed]

Shinomori, K., Spillman, L., & Werner, J. S. (1999). S-cone signals to temporal OFF-channels: Asymmetrical connections to postreceptoral chromatic mechanisms. *Vision Research, 39,* 39–49. [PubMed]

Smith, V. C., & Pokorny, J. (1975). Spectral sensitivity of the foveal cone photopigments between 400 and 500 nm. *Vision Research, 15,* 161–171. [PubMed]

Smith, V. C., & Pokorny, J. (1995). Chromatic-discrimination axes, CRT phosphor spectra, and individual variation in color vision. *Journal of the Optical Society of America A, Optics, Image Science, and Vision, 12,* 27–35. [PubMed]

Szmajda, B. A., Buzas, P., Fitzgibbon, T., & Martin, P. R. (2006). Geniculocortical relay of blue-off signals in the primate visual system. *Proceedings of the National Academy of Sciences of the United States of America, 103,* 19512–19517. [PubMed] [Article]

Thibos, L. N. (1987). Calculation of the influence of lateral chromatic aberration on image quality across the visual field. *Journal of the Optical Society of America A, Optics and Image Science, 4,* 1673–1680. [PubMed]

Thibos, L. N., Cheney, F. E,., & Walsh, D. J. (1987). Retinal limits to the detection and resolution of gratings. *Journal of the Optical Society of America A, Optics and Image Science, 4,* 1524–1529. [PubMed]

Thibos, L. N., Walsh, D. J., & Cheney, F. E. (1987). Vision beyond the resolution limit: Aliasing in the periphery. *Vision Research, 27,* 2193–2197. [PubMed]

Thomas, J. P. (1985). Detection and identification: How are they related? *Journal of the Optical Society of America A, Optics and Image Science, 2,* 1457–1467. [PubMed]

Valberg, A., Lee, B. B., & Tigwell, D. A. (1986). Neurones with strong inhibitory S-cone inputs in the macaque lateral geniculate nucleus. *Vision Research, 26,* 1061–1064. [PubMed]

Van Norren, D., & Vos, J. J. (1974). Spectral transmission of the human ocular media. *Vision Research, 14,* 1237–1243. [PubMed]

Vassilev, A., Ivanov, I., Zlatkova M. B., & Anderson, R. (2005). Human S-cone vision: Relationship between perceptive field and ganglion cell dendritic field. *Journal of Vision, 5*(10):6, 823–833, http://journalofvision.org/5/10/6/, doi:10.1167/5.10.6. [PubMed] [Article]

Vassilev, A., Mihaylova, M. S., Racheva, K., Zlatkova, M., & Anderson, R. S. (2003). Spatial summation of S-cone ON and OFF signals: Effects of retinal eccentricity. *Vision Research, 43,* 2875–84. [PubMed]

Vassilev, A., Zlatkova, M., Manahilov, V., Krumov, A., & Schaumberger, M. (2000). Spatial summation of blue-on-yellow light increments and decrements in human vision. *Vision Research, 40,* 989–1000. [PubMed]

Wassle, H., & Boycott, B. B. (1991). Functional architecture of the mammalian retina. *Physiological Review, 71,* 447–480. [PubMed]

Werner, J. S., Donnelly, S. K., & Kliegl, R. (1987). Aging and human macular pigment density. Appended with translations from the work of Max Schultze and Ewald Hering. *Vision Research, 27,* 257–268. [PubMed]